


Ferruginol Inhibits Non–Small Cell Lung Cancer Growth by Inducing Caspase-Associated Apoptosis

Integrative Cancer Therapies
2015, Vol. 14(1) 86–97
© The Author(s) 2014
Reprints and permissions:
sagepub.com/journalsPermissions.nav
DOI: 10.1177/1534735414555806
ict.sagepub.com


Shang-Tse Ho, MS¹, Yu-Tang Tung, PhD¹, Yueh-Hsiung Kuo, PhD²,
Chi-Chen Lin, PhD¹, and Jyh-Horng Wu, PhD¹

Abstract

Purpose. The anti–lung cancer effect of *Cryptomeria japonica* leaf extractive and its active phytochemical was evaluated using in vitro and in vivo assays. **Experimental Design.** The anti–lung cancer mechanism was investigated using flow cytometry and western blot analyses, and the antitumor activity was evaluated in a xenograft animal model. **Results.** MTT assay indicated that the cytotoxic effects of ferruginol in A549 and CL1-5 cells were dose-dependent. According to the results of cell cycle and annexin V/PI analyses, the sub-G₁ population and annexin V binding in the 2 cell lines were increased after ferruginol treatment. The results of western blot analyses revealed that the cleaved forms of caspase 3, 8, 9, and poly(ADP-ribose) polymerase were activated after ferruginol treatment in A549 and CL1-5 cells. Moreover, the expression of the anti-apoptotic protein Bcl-2 was decreased, while the expression of the pro-apoptotic protein Bax was elevated, after ferruginol treatment in both lung cancer cell lines. These results indicated that ferruginol acted via a caspase-dependent mitochondrial apoptotic pathway in the 2 cell lines. Intraperitoneal administration of ferruginol significantly suppressed the growth of subcutaneous CL1-5 xenografts. **Conclusions.** The findings of the present study provided insight into the molecular mechanisms underlying ferruginol-induced apoptosis in non–small cell lung cancer (NSCLC) cells, indicating that this compound may be a potential candidate drug for anti-NSCLC.

Keywords

Cryptomeria japonica, phytochemical, lung cancer, NSCLC, ferruginol, caspase, apoptosis

Introduction

Lung cancer is one of the most common cancers globally and accounts for more than one quarter of all cancer deaths.¹ Based on cancer cell growth features, there are 2 main types of lung cancer: small cell lung cancer (SCLC) and non–small cell lung cancer (NSCLC). NSCLC accounts for approximately 80% of all lung cancers and includes 3 major histologic subtypes: squamous cell carcinoma, adenocarcinoma, and large cell lung cancer.^{2,3} The typical symptoms of lung cancer are invasion and metastasis to other organs, and they have been associated with high mortality. The average 5-year survival rate of lung cancer patients is approximately 15%, and in recent decades, the survival rate and early diagnosis have only slightly improved.^{4,6}

Surgery, radiation, and chemotherapy are common therapeutic approaches for lung cancer, but therapy resistance and certain side effects of these approaches have limited their application.^{7,8} In light of the aforementioned issues, many researchers have attempted to search for novel anticancer agents from natural products due to their cytotoxic potential and relative safety in the human body.^{9–12} Recently,

the anticancer activity and related mechanisms of natural products have been widely reported.^{13–15}

Cryptomeria japonica, also called Japanese cedar, is a well-known plantation tree species that is of important industrial value for craft, building, and construction materials in Taiwan. The leaf extract of *C. japonica* has been reported to have excellent bioactivities, including cytotoxic, antioxidant, antifungal, anti-inflammatory, antibacterial, and hepatoprotective effects.^{16–19} According to previous reports, *C. japonica* extract is strongly cytotoxic and may be a potential candidate for use as a novel natural anticancer

¹National Chung Hsing University, Taichung, Taiwan

²China Medical University, Taichung, Taiwan

Corresponding Authors:

Jyh-Horng Wu, Department of Forestry, National Chung Hsing University, Taichung 402, Taiwan.
Email: eric@nchu.edu.tw

Chi-Chen Lin, Institute of Biomedical Sciences, National Chung Hsing University, Taichung 402, Taiwan.
Email: lincc@nuhu.edu.tw

agent.¹⁶ However, the active phytochemicals and their underlying anti-lung cancer mechanisms remain unclear. Thus, the anti-lung cancer effects of *C japonica* extract and its active phytochemicals were evaluated in 2 NSCLC cell lines: A549 and CL1-5 human lung adenocarcinoma cells. On the other hand, it is well known that ferruginol is one of the major phytochemicals in *C japonica* extract,²⁰ and it had been reported with in vitro cytotoxicity in human cancer cell lines.²¹ In the present study, the anti-lung cancer mechanism of the active phytochemical, ferruginol, from *C japonica* was investigated using flow cytometry and western blot analyses, and the antitumor activity was evaluated in a xenograft animal model. Additionally, to the best of our knowledge, this is the first time that ferruginol has been isolated from the methanolic leaf extract of *C japonica*.

Materials and Methods

Chemicals and Reagents

3-(4,5-Dimethylthiazol-2-yl)-2,5-diphenyltetrazolium bromide (MTT), dimethyl sulfoxide (DMSO), 2-[4-(2-hydroxyethyl)piperazin-1-yl]ethanesulfonic acid (HEPES), propidium iodide (PI), and Triton X-100 were purchased from Sigma Chemical Co (St Louis, MO). RPMI medium 1640, Dulbecco's modified Eagle's medium (DMEM), fetal bovine serum (FBS), and trypsin-ethylenediaminetetraacetic acid (trypsin-EDTA) were obtained from Gibco (Grand Island, NY). Antibodies cleaved caspase-3, cleaved caspase-8, cleaved caspase-9, and cleaved-poly (ADP-ribose) polymerase (PARP) antibodies were purchased from Cell Signaling Technology Inc (Danvers, MA). Bax, Bcl-2, Smac, survivin, XIAP, and β -actin antibodies were purchased from Abcam (Cambridge, MA). All the other chemicals and solvents used in this experiment were of analytical grade.

Plant Materials, Extraction, and Isolation

Cryptomeria japonica leaves were collected from the Hui-Sun Forest Station of National Chung Hsing University in Taichung County. The species was identified by Dr Yen-Hsueh Tseng of the National Chung Hsing University. The leaves of *C japonica* were cleaned with tap water, dried, and extracted twice using methanol for 1 week at room temperature (25°C). The methanolic extract was decanted, filtered under vacuum, concentrated in a rotary evaporator, and then lyophilized. The samples were dissolved in H₂O, *n*-hexane was then added, and the mixture was vigorously stirred. The organic layer was removed to yield a hexane-soluble fraction. Some insoluble matter was retained in the aqueous phase, to which ethyl acetate (EtOAc) was added and stirred. Similarly, the organic layer was removed to yield an

EtOAc-soluble fraction. Subsequently, *n*-butanol (BuOH) was added to the aqueous phase, stirred, and the layers separated to give BuOH- and water-soluble fractions, respectively. The hexane-soluble fraction of *C japonica* was loaded onto a chromatography column (Geduran Si-60, Merck, Darmstadt, Germany), eluted using a gradient of EtOAc/*n*-hexane solvent systems, and 10 subfractions were collected. The cytotoxicity of each subfraction was determined using an MTT assay. The active phytochemical, ferruginol (Figure 1A), from subfraction 1 was further isolated and purified via semipreparative high-performance liquid chromatography (HPLC) using a PU-2080 pump (Jasco, Tokyo, Japan) equipped with an RI-2031 detector (Jasco, Tokyo, Japan) and a 5 μ m Luna silica column (250 \times 10.0 mm internal diameter; Phenomenex, Torrance, CA). EtOAc/*n*-hexane (2/98, v/v) was used as an isocratic mobile phase at a flow rate of 4 mL/min. The structure of ferruginol was identified using nuclear magnetic resonance imaging (Bruker Avance 400 MHz FTNMR Spectrometer, Rheinstetten, Germany). All the spectral data were consistent with those reported in the literature.²²

Cell Culture

The A549 and CL1-5 human NSCLC cell lines were cultured in RPMI medium 1640 and DMEM that had been supplemented with 10% FBS and 1% antibiotic antimycotic, respectively. The cultures were maintained in a humidified incubator containing 5% CO₂ at 37°C.

Cytotoxicity Assays

The cytotoxic effects of *C japonica* leaf extract and its derived fractions, subfractions, and ferruginol in lung cancer cells were measured using the MTT assay. A549 and CL1-5 cells were seeded onto 24-well plates at densities of 1×10^4 cells/well for 24 hours. After 24 hours, the test samples (50 μ g/mL of extracts, and 100, 80, 60, 40, and 20 μ M of ferruginol) were added to a 24-well plate followed by 24-hour incubation. DMSO alone was used as the control in this experiment. Then, the supernatant was removed and 200 μ L of MTT solution (1 mg/mL) was added to each well for 4 hours. The extent of MTT reduction was quantified by measuring the absorbance at 570 nm using an ELISA reader (Labsystems Multiskan MS, Helsinki, Finland). To quickly screen the cytotoxic potential of each fraction, the extract and soluble fractions were assessed at a concentration of 50 μ g/mL.

Cell Cycle Analyses

The cells (at a density of 1.5×10^5 cells) were seeded onto 6-well plates for 24 hours. The cells were then treated with 40, 60, and 80 μ M of ferruginol for 24 hours, and 80 μ M of

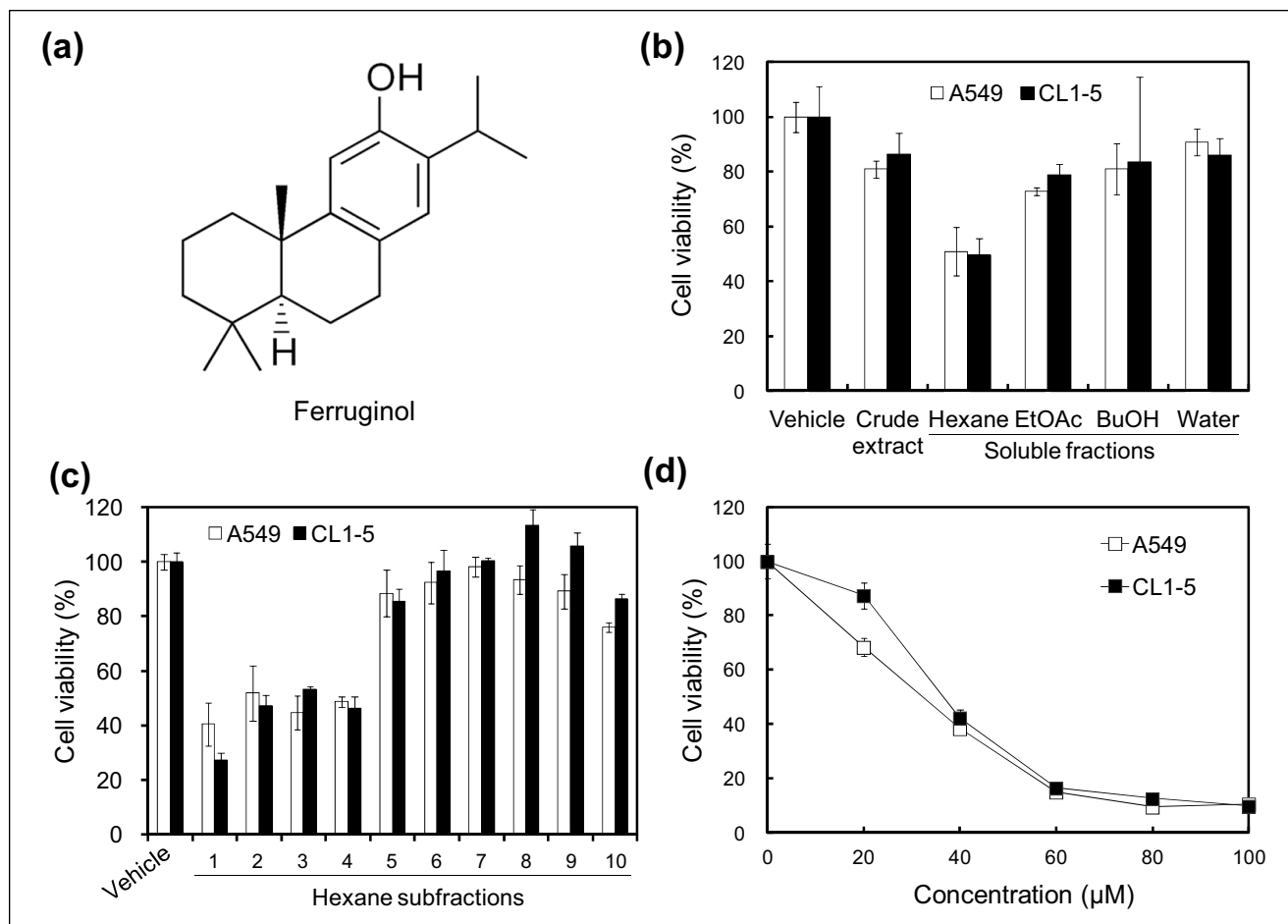


Figure 1. The cytotoxic effects of the *Cryptomeria japonica* extract and its active phytochemical in A549 and CL1-5 cells. (A) Chemical structure of ferruginol. (B) Viability of A549 and CL1-5 cells after treatment with 50 µg/mL of *C. japonica* leaf extract and its derived soluble fractions for 24 hours. (C) Viability of A549 and CL1-5 cells after treatment with 50 µg/mL of hexane subfractions 1 to 10 for 24 hours. (D) Viability of A549 and CL1-5 cells after ferruginol treatment for 24 hours. The results represent the means \pm SD ($n = 3$).

ferruginol for 6, 12, and 24 hours followed by cell collection via centrifugation and then washed with ice-cold phosphate buffered saline (PBS) twice. The cell pellets were mixed with 75% ethanol at -20°C overnight. The cells were then centrifuged and resuspended in 400 µL of PI staining solution (2 mg/mL of RNase, 1 mg/mL of PI, and 0.5% Triton X-100) for 30 minutes at room temperature in the dark, after which the cells were analyzed using flow cytometry (FACSCalibur, BD BioSciences, Franklin Lakes, NJ). The distributions and percentages of cells in the sub- G_1 , G_0/G_1 , S, and G_2/M phases of the cell cycle were analyzed using WinMDI software (Scripps Research Institute, La Jolla, CA).

Annexin V/PI Staining Assays

The apoptotic patterns of lung cancer cells after ferruginol treatment were determined using an Annexin V-FITC Apoptosis Detection Kit (BioVision, Milpitas, CA). A549

and CL1-5 cells were seeded onto 6-well plates at densities of 1.5×10^5 cells/well for 24 hours and were then exposed to 40, 60, and 80 µM of ferruginol for 6 hours. The cells were harvested by trypsinization and washed twice with PBS. The cell suspensions were then incubated with 2 µL of annexin V-FITC and 2 µL of PI in 100 µL of binding buffer (0.01 M HEPES, pH 7.4; 0.14 M NaCl; 2.5 mM CaCl_2) for 10 minutes at room temperature in the dark. The cells were immediately evaluated using flow cytometry.

Mitochondrial Membrane Potential Assays

To determine the mitochondrial membrane potential of A549 and CL1-5 cells after ferruginol treatment, a specific cationic dye for mitochondria, JC-1 (Invitrogen, Carlsbad, CA), was used. In this assay, 1.5×10^5 cells were seeded onto 6-well plates for 24 hours. Then, the cells were exposed to 40, 60, and 80 µM of ferruginol for 6 hours, harvested by trypsinization, and washed twice with PBS. The cell

suspensions were then incubated with 2 μL of JC-1 dye (10 mg/mL) in 1 mL of PBS for 15 minutes at 37°C and washed in PBS. The mitochondrial membrane potential was determined using flow cytometry.

Cytochrome *c* Level Analyses

Cytochrome *c* levels in A549 and CL1-5 cells after ferruginol treatment were analyzed using flow cytometry. Briefly, 1.5×10^5 cells were seeded onto 6-well plates for 24 hours and then treated with 80 μM ferruginol for 1, 3, and 6 hours. Harvested cells were incubated for 5 minutes on ice in 100 μL of digitonin buffer (80 mM potassium chloride [KCl], 50 ng/mL of digitonin, and 1 mM EDTA in PBS). The permeabilized cells were fixed with 4% paraformaldehyde in PBS, washed with 0.1% bovine serum albumin (BSA) in PBS, and incubated for 1 hour in blocking buffer (3% BSA and 0.05% saponin in PBS). The cells were then stained with anti-fluorescein isothiocyanate (FITC) cytochrome *c* antibody (BD Pharmingen, Franklin Lakes, NJ) for 1 hour at 4°C in the dark, followed by washing, centrifugation, and resuspension. Fluorescence was detected using flow cytometry.

Western Blot Analyses

Whole cells proteins were lysed in RIPA buffer containing 10% proteinase inhibitor and boiled on a heated plate at 95°C for 5 minutes. Protein concentrations were measured using a BCA Protein Assay. Proteins (30–60 μg for the different experiments) were loaded at different percentages onto SDS-PAGE gels for gel electrophoresis. Then, the proteins were transferred to a PVDF membrane and blocked (5% nonfat milk in TBST buffer) for 1 hour. The membranes were incubated with various primary antibodies (cleaved caspase-3, cleaved caspase-8, cleaved caspase-9, cleaved-PARP, Bax, Bcl-2, Smac, survivin, XIAP, and β -actin). After washing, the blots were incubated with HRP-labeled mouse or rabbit secondary antibodies (Jackson ImmunoResearch Laboratories, West Grove, PA) for 2 hours. The signals of the blots were then developed using an enhanced chemiluminescence (ECL) system and analyzed using the LAS3000 system (Fujifilm, Tokyo, Japan).

In Vivo Antitumor Activity

CL1-5 cells at a density of 3×10^6 were subcutaneously (sc) injected into the flanks of 4- to 6-week-old male nude mice. The CL1-5 xenograft mice were subdivided into groups of 5 mice. When the mean tumor volume was 50 mm^3 (approximately 10 days after tumor inoculation), therapy was initiated. Ferruginol was dissolved in 0.5% DMSO and injected intraperitoneally (ip) at 100 $\mu\text{mol}/\text{kg}$ of BW daily. Control mice were ip injected daily with ddH₂O containing 0.5%

DMSO. The experimental period was 32 days, following 22 days of ferruginol administration. The tumor weights were recorded and tumor volumes were calculated as the length \times width \times thickness \times 0.5 and expressed in mm^3 .

Immunohistochemistry (IHC) With Xenograft Tumor Tissue

Tumor tissue was obtained from CL1-5 xenograft mice and detected the expression of the cleaved caspase-3 protein. The tumor tissue slides were deparaffinized and dehydrated with xylene as well as ethanol, respectively. The IHC staining was according to the manufacturer's instruction protocol (NovoLink Max Polymer Detection System, Leica, Newcastle Upon Tyne, UK).

Statistical Analyses

The results are expressed as the means \pm SD ($n = 3$) or means \pm SEM ($n = 5$). Statistical comparisons between 2 groups of data were made using an unpaired 1-tailed Student's *t* test, and *P* values $< .05$ were considered to be significant.

Results

Cryptomeria japonica Leaf Extract Exhibits Cytotoxic Effects in Human NSCLC Cells

To determine the cytotoxic effects of *C. japonica* leaf extract and its soluble fractions in human NSCLC cells, A549 and CL1-5 cells were treated with *C. japonica* leaf extract and its derived soluble fractions for 24 hours and the MTT assay was used to measure cell viability. Among the *C. japonica* leaf extract and its derived soluble fractions, the hexane-soluble fraction was the most cytotoxic in A549 (56.4%) and CL1-5 (56.0%) cells at a concentration of 50 $\mu\text{g}/\text{mL}$ (Figure 1B). The hexane-soluble fraction of the *C. japonica* leaves decreased cell viability in both A549 and CL1-5 cells in a dose-dependent manner, and the IC₅₀ values in both cell lines were approximately 50 $\mu\text{g}/\text{mL}$ (data not shown). These results revealed that the hexane-soluble fraction of *C. japonica* leaves had cytotoxic potential and may be the source of a novel natural antitumor agent. Thus, the hexane-soluble fraction was further derived into 10 subfractions using column chromatography. Of these, subfraction 1 exhibited the highest cytotoxicity at a concentration of 50 $\mu\text{g}/\text{mL}$, and the cell viabilities of A549 and CL1-5 were 40% and 27%, respectively (Figure 1C). Based on a bioactivity-guided isolation principle, the bioactive phytochemical, ferruginol, was further isolated via HPLC from subfraction 1. In addition, the cytotoxic effects of ferruginol were further determined. As shown in Figure 1D, the cytotoxicity of ferruginol increased as its concentration increased, and the IC₅₀ values

in A549 and CL1-5 cells were 33.0 μM and 39.3 μM , respectively.

Ferruginol Induced Sub-G₁ Phase and Apoptotic Cell Death in Human NSCLC Cells

To determine the cell cycle inhibitory effects of ferruginol in A549 and CL1-5 cells, the cells were subjected to flow cytometric analyses after ferruginol treatment. The results of the dose–response and time course cell cycle distribution analyses in A549 and CL1-5 cells after ferruginol treatment are shown in Figure 2. In comparison to the control group, the sub-G₁ population of the 80 μM ferruginol-treated group significantly increased at 24 hours (Figure 2A). The effects of exposure to 80 μM ferruginol for different time periods in A549 and CL1-5 cells were also determined. As shown in Figure 2B, the sub-G₁ peak increased in A549 and CL1-5 cells after treatment with ferruginol for 6, 12, and 24 hours. In addition, the sub-G₁ peak was considered to be an apoptosis-related peak based on the cell cycle analyses. To confirm the results of the cell cycle analyses in A549 and CL1-5 cells after ferruginol treatment, annexin V/PI staining was also performed in this study. A549 and CL1-5 cells were treated with 0, 40, 60, and 80 μM of ferruginol for 6 hours, and annexin V/PI staining was determined using a flow cytometer. As shown in Figure 3A, the percentage of annexin V positive A549 and CL1-5 cells increased in a dose-dependent manner. These results revealed that ferruginol may potentially be an apoptosis inducer in A549 and CL1-5 cells. The mitochondria play a critical and central role in the apoptotic process due to their involvement in the intrinsic and extrinsic apoptotic pathways.²³ To determine whether mitochondrial dysfunction was involved in ferruginol-induced apoptosis in A549 and CL1-5 cells, the effects of ferruginol on mitochondrial membrane potential ($\Delta\psi\text{m}$) were analyzed via JC-1 staining and determined using a flow cytometer. The cells were treated with ferruginol for 6 hours and mitochondrial dysfunction was observed to increase in a dose-dependent manner in A549 and CL1-5 cells (Figure 3B), suggesting that the mitochondria-regulated apoptotic pathway was induced in A549 and CL1-5 cells after treatment with ferruginol. Accordingly, mitochondrial cytochrome *c* release induces downstream caspase activation, which is a key step for apoptosis initiation.²⁴ To assess the role of cytochrome *c* in ferruginol-induced NSCLC cell death, A549 and CL1-5 cells were exposed to 80 μM ferruginol for 1, 3, and 6 hours, and cytochrome *c* release was then analyzed using a flow cytometer. As shown in Figure 3C, cytochrome *c* release increased as ferruginol treatment duration increased in both A549 and CL1-5 cells. Based on the results outlined above, mitochondrial dysfunction may play an important role in ferruginol-induced NSCLC cell apoptosis.

Ferruginol Inhibited Human NSCLC Cell Growth via a Caspase-Dependent Pathway

Activation of caspase family proteins plays a crucial role in apoptosis. Two main pathways, namely, the intrinsic and extrinsic pathways, are involved in caspase-related apoptosis. To investigate the molecular mechanisms underlying ferruginol-induced A549 and CL1-5 cell apoptosis, apoptosis-related proteins were examined via western blot analyses. The results of the western blot analyses revealed that the cleaved forms of caspase 3, 8, 9, and poly(ADP-ribose) polymerase (PARP) were activated after ferruginol treatment in the A549 and CL1-5 cell lines (Figure 4). Based on these results, ferruginol may induce apoptosis via both the intrinsic and extrinsic pathways. Moreover, the expression of the anti-apoptotic protein Bcl-2 was decreased, while the expression of the pro-apoptotic protein Bax was elevated, after ferruginol treatment in both lung cancer cell lines (Figure 5A). The Bcl-2/Bax ratio is also an important index to assess the regulatory effect of these proteins in the cell death process. As shown in Figure 5B, the Bcl-2/Bax ratios of A549 and CL1-5 cells were decreased in a dose-dependent manner after ferruginol treatment. In A549 cells, the Bcl-2/Bax ratios were 1, 0.64, 0.37, and 0.30 for 0, 40, 60, and 80 μM ferruginol treatment groups, respectively. The similar tendency was also found in CL1-5 cells and indicated that ferruginol decreased the Bcl-2/Bax ratio as well as induced the mitochondrial dysfunction in lung cancer cell lines. In contrast, the activities of caspase family proteins were also regulated by IAP family proteins. Thus, the expression of survivin and XIAP were also determined using western blot analyses. As shown in Figure 5A, the expression of IAP family proteins was decreased after ferruginol treatment in A549 and CL1-5 cells. Additionally, the expression of Smac was enhanced after ferruginol treatment in 2 cell lines. These results indicated that ferruginol exhibited caspase-dependent mitochondrial apoptotic pathway activation in the 2 cell lines.

Ferruginol Inhibits CL1-5 Tumor Growth in a Subcutaneous Xenograft Animal Model

The results of the *in vitro* assays outlined above revealed that ferruginol was a potentially cytotoxic phytochemical. However, to the best of our knowledge, the *in vivo* antitumor effect of ferruginol remained unclear. To determine the *in vivo* antitumor effect of ferruginol, male nude mice were *sc* inoculated with CL1-5 cells, and the mice were then injected *ip* with 100 $\mu\text{mol/kg}$ of BW of ferruginol 10 days after tumor inoculation. As shown in Figure 6A–C, ferruginol alleviated tumor growth in nude mice, as evidenced by both tumor volume and weight. Furthermore, IHC staining (for cleaved caspase 3) was performed to confirm the ability of ferruginol to induce apoptosis in tumor xenograft mice.

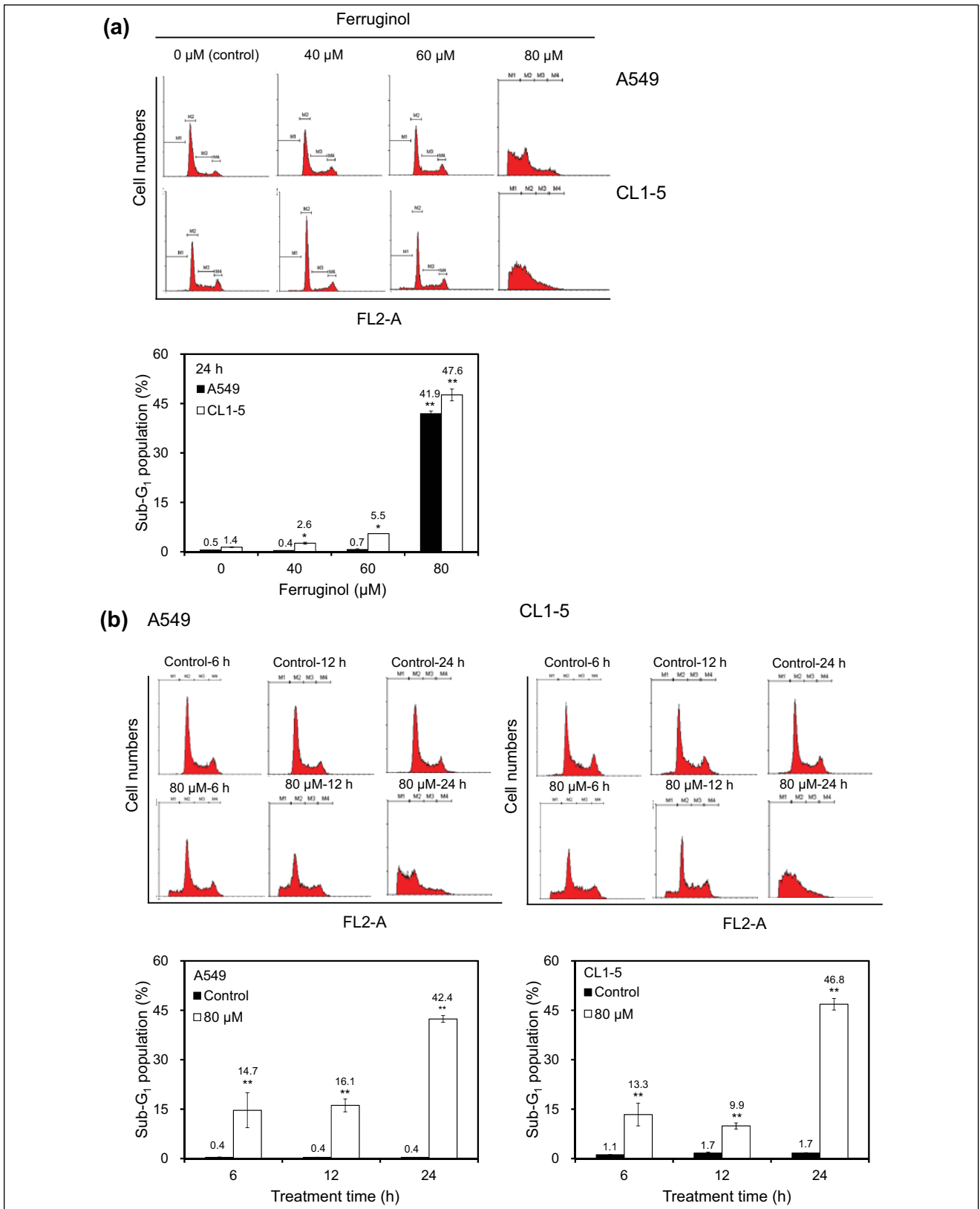


Figure 2. Effects of ferruginol on cell-cycle distribution in A549 and CL1-5 cells. (A) Cell cycle analyses of A549 and CL1-5 cells after 40, 60, and 80 μM ferruginol treatment for 24 hours. (B) cell cycle analyses of A549 and CL1-5 cells after 80 μM ferruginol treatment for 6, 12, and 24 hours. These results are representative of 3 independent experiments in which similar results were obtained. **P* < .05 and ***P* < .01 for the ferruginol-treated groups compared to the vehicle-treated control group.

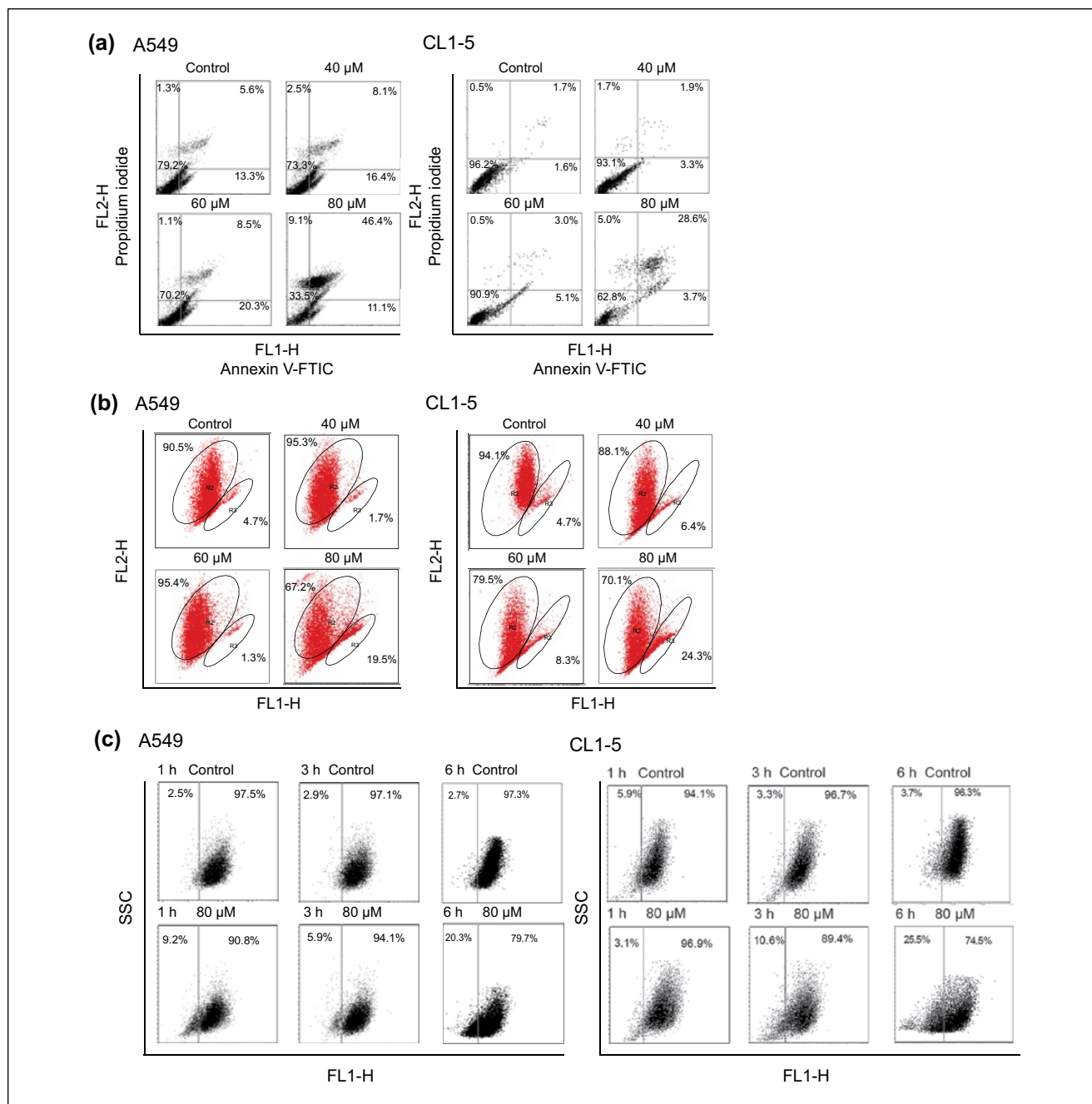


Figure 3. Ferruginol-induced apoptosis and mitochondrial dysfunction in A549 and CL1-5 cells.

Cells, depicted as squares, are plotted as red fluorescence intensity (FL2-H) versus green fluorescence intensity (FL1-H). (A) Annexin V and PI analyses in A549 and CL1-5 cells after 40, 60, and 80 μ M ferruginol treatment for 6 hours. (B) Mitochondrial membrane potential analyses in A549 and CL1-5 cells after 40, 60, and 80 μ M ferruginol treatment for 6 hours. (C) Cytochrome c release analyses in A549 and CL1-5 cells after ferruginol treatment for 1, 3, and 6 hours. These results are representative of 2 to 3 independent experiments in which similar results were obtained.

As shown in Figure 6D, a higher proportion of cleaved caspase 3–positive apoptotic cells was found in mice after ferruginol treatment than after vehicle treatment. These results indicated that ferruginol also inhibited CL1-5 cell growth in tumor xenograft mice and may be a potential candidate for novel potent antitumor agent development.

Discussion

Cryptomeria japonica is a well-known forest tree species that is of important industrial value in Taiwan. The cytotoxic effects of *C. japonica* extract have been well characterized. Cha and Kim²⁵ reported that the essential oil from *C.*

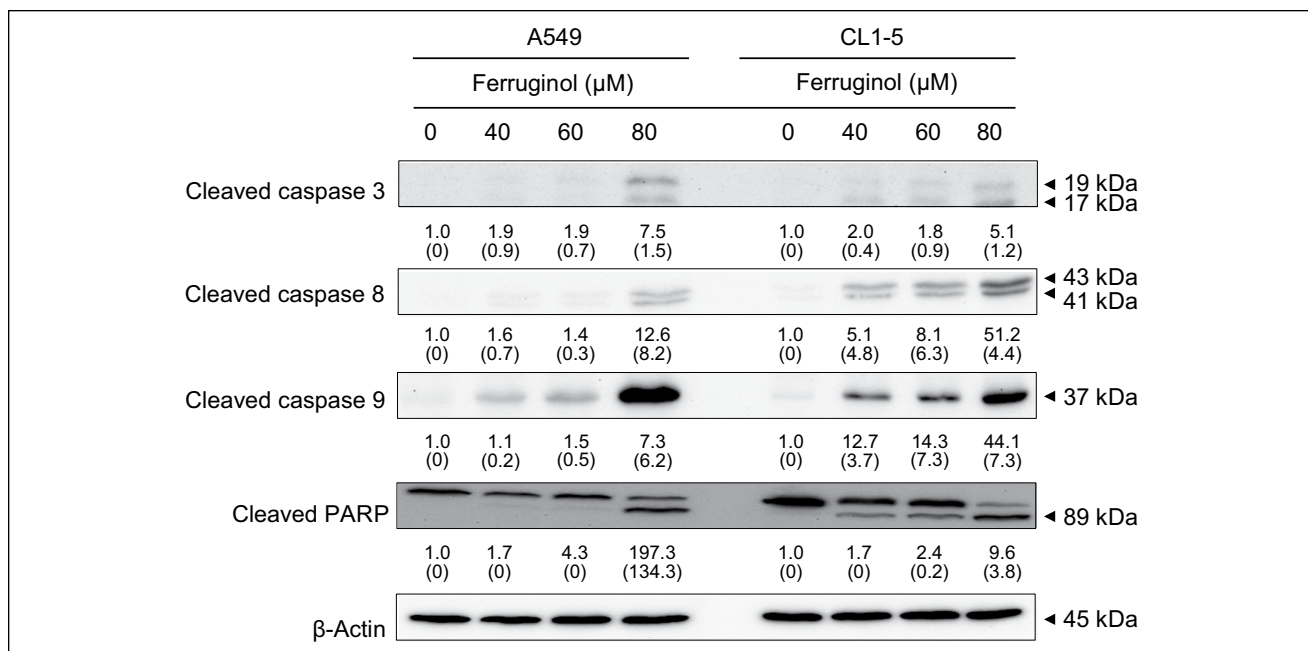


Figure 4. Ferruginol activated caspase family protein expression in A549 and CL1-5 cells after 40, 60, and 80 μM ferruginol treatment for 6 hours.

These results are representative of 3 independent experiments in which similar results were obtained. Numbers below each panel indicate the average relative densities to control group quantified by Image J software, and SD values are shown in parentheses.

japonica induces apoptosis in KB cells (a human oral carcinoma cell) through a mitochondrial stress- and caspase-dependent pathway. A report by Lin et al²⁶ indicated that 6-hydroxy-5,6-dehydrosugirol, a diterpene isolated from the stem bark of *C japonica*, reduced the viability of 2 prostate cancer cell lines (LNCaP and 22Rv1) by inducing caspase 3, 7, and PARP activities. In addition, 6-hydroxy-5,6-dehydrosugirol also induces G₁ phase cell cycle arrest in LNCaP and 22Rv1 cells. Yoshikawa et al²⁷ reported that sugikurojin G, 7β-methoxydeoxocryptojaponol, and 5,6-dehydrosugirol, 3 compounds that were isolated from the bark of *C japonica*, were cytotoxic in the HL-60 and HCT-15 cancer cell lines. The immunoregulatory activities of the phytochemicals and extracts of *C japonica* have also been reported.²⁸ Based on the results outlined above, the bioactivities of *C japonica* extracts have been determined, especially those of the diterpene compounds.^{27,28} Although many bioactivity studies of *C japonica* extracts have been reported, the anti-cancer activities and related molecular mechanisms of these extracts remain unclear. In the present study, we described the cellular and molecular events underlying the growth inhibitory effects of *C japonica* extracts in human NSCLC cells.

Two major apoptotic pathways, namely, the extrinsic and intrinsic pathways, are mediated by caspase family proteins. The extrinsic apoptotic pathway is initiated by death receptor activation, including TNF-R1, CD95, and the TNF-related apoptosis-inducing ligands, (TRAIL)-R1 and

(TRAIL)-R2. The activity of caspase 8 is then enhanced, followed by the induction of the downstream apoptosis cascade. Accordingly, the other apoptotic pathway (the intrinsic pathway) is more closely related to mitochondrial dysfunction and mitochondrial membrane proteins, such as Bcl-2 family protein expression.^{29,30} In the present study, we found that ferruginol affected mitochondrial membrane potential and enhanced cytochrome *c* release in A549 and CL1-5 cells, suggesting that the cancer cell growth inhibitory effect of this phytochemical may be due to the induction of mitochondrial dysfunction. Additionally, expression of the anti-apoptotic protein Bcl-2 decreased, whereas expression of the pro-apoptotic protein Bax increased in A549 and CL1-5 cells after treatment with ferruginol (Figure 5). The results revealed that mitochondria-mediated apoptosis was induced by ferruginol in A549 and CL1-5 cells. Additionally, other diterpenes have been reported to have inhibitory effects on tumor cell growth due to regulation of Bcl-2 family protein expression.³¹ Caspase family proteins play different roles in the apoptotic process; these proteins initially become activated, and cell death events are also triggered.³² In the present study, caspase 8 and 9 cleavage increased, activating downstream caspase 3 and PARP cleavage in A549 and CL1-5 cells after ferruginol treatment, especially at high doses. These results indicated that the inhibitory effects of ferruginol may be mediated via the induction of caspase-dependent apoptosis and both the intrinsic and extrinsic pathways may be involved.

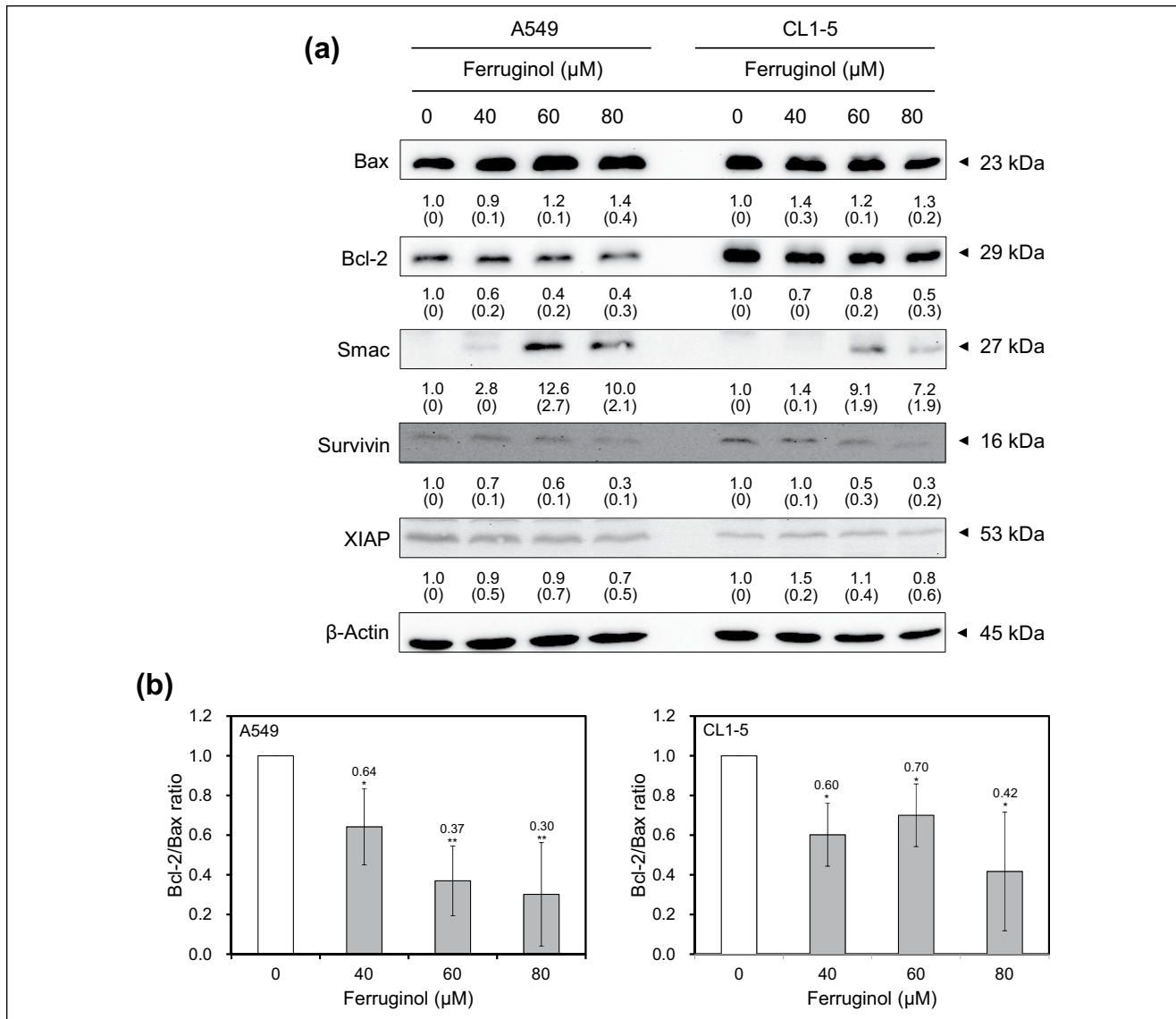


Figure 5. (A) Bcl-2 and IAP family protein expression in A549 and CL1-5 cells after 40, 60, and 80 μM ferruginol treatment for 6 hours. These results are representative of 2 to 3 independent experiments in which similar results were obtained. Numbers below each panel indicate the average relative densities to control group quantified by Image J software, and SD values are shown in parentheses. (B) The Bcl-2/Bax ratios of A549 and CL1-5 cells treatment with various concentrations of ferruginol. * $P < .05$ and ** $P < .01$ for the ferruginol-treated groups compared to the vehicle-treated control group.

Inhibitor of apoptosis proteins (IAPs) are a family of proteins that downregulate the apoptotic response by inhibiting caspases. X-linked IAP (XIAP) is one of the well-known members of the IAP family, and XIAP has been reported to have anti-apoptotic activity due to its activity as a potent natural caspase inhibitor.^{32,33} Survivin is also an IAP family member that is active against some apoptotic stimuli, such as Fas, high levels of Bax, and caspase expression as well as chemotherapeutic drugs, and a recent study revealed that XIAP and survivin are highly expressed in many human tumor subtypes.³⁴ Thus, decreasing the expression of IAPs, such as XIAP and survivin, may promote

apoptotic events. In the present study, the IAP family protein XIAP and survivin were downregulated in A549 and CL1-5 cells after ferruginol treatment. Smac, an inhibitor of IAPs proteins, also plays a role in apoptosis process. The expression of Smac was elevated after ferruginol treatment in this study. This result indicated that ferruginol enhanced Smac expression, then inhibited the IAPs, and consequently induced apoptosis in A549 and CL1-5 cells. To the best of our knowledge, this study is the first report describing the interaction between IAP family proteins and ferruginol treatment in NSCLC cells. In the present study, the results indicated that ferruginol induced apoptosis in A549 and

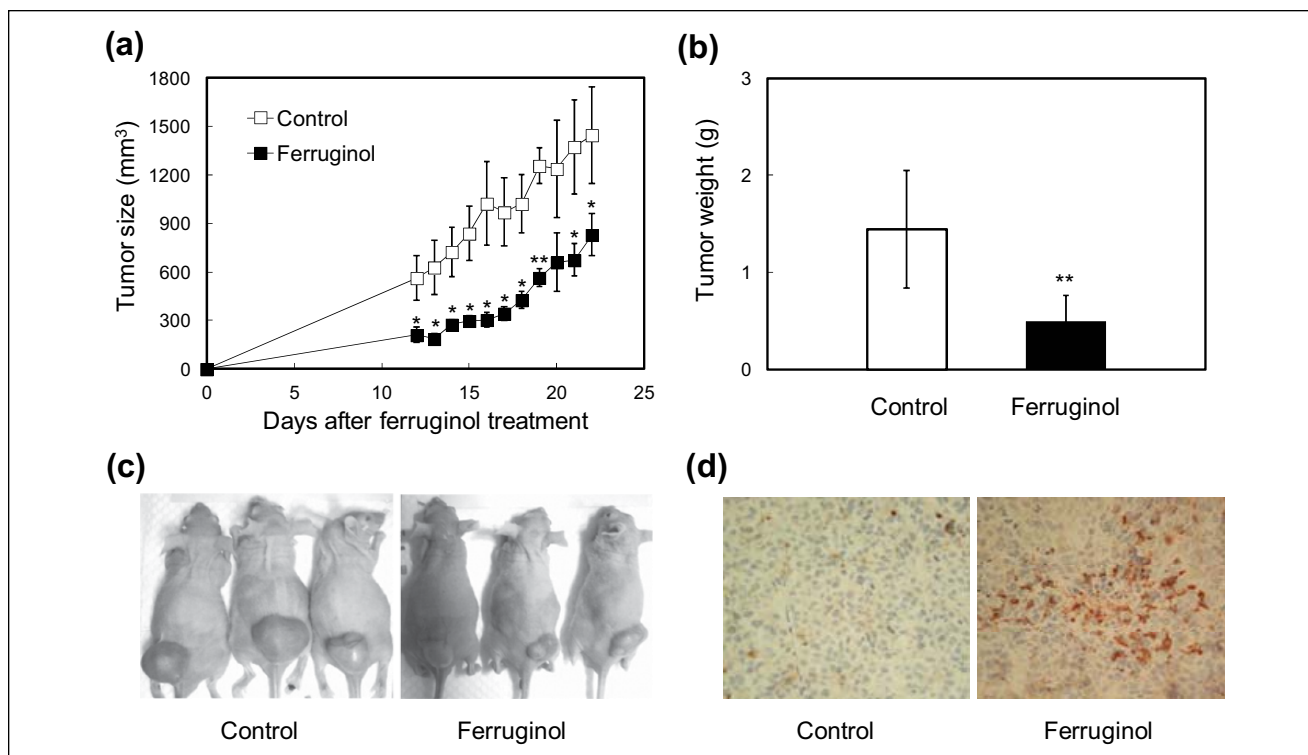


Figure 6. Effects of ferruginol (100 μmol/kg of BW) on CL1-5 xenograft tumor volume at different days of treatment (A), tumor weight measured at 22 days after ferruginol treatment (B), human lung tumor xenograft growth in nude mice with/without ferruginol treatment at 22 days after ferruginol treatment (C), and IHC staining (of cleaved caspase 3) in the vehicle-treated control and ferruginol-treated groups (D). The results represent the means ± SEM (n = 5). *P < .05 and **P < .01 for the ferruginol-treated groups compared to the vehicle-treated control group.

CL1-5 cells by activating caspase family proteins and inhibiting Bcl-2, survivin, and XIAP expression, thereby causing cell death by both the extrinsic and intrinsic apoptosis pathways (Figure 7).

Mouse models of cancer therapy have been widely used to screen for new anticancer agents in the fields of natural products and biomedicine. Two of the commonly used models are the murine tumor model and the human tumor xenograft model.³⁵ In the present study, we used a CL1-5 xenograft mouse model to assess the anti-lung cancer effects of ferruginol. Tumor size and weight in xenograft mice were decreased after ferruginol treatment. The results of IHC staining revealed that caspase 3 cleavage was promoted in the ferruginol treatment group, suggesting that ferruginol induced apoptosis in the xenograft model. These findings provided valuable evidence supporting the potential use of ferruginol in anti-lung cancer agent development and indicated that ferruginol may be a new candidate for lung cancer treatment.

Conclusions

In the present study, the in vitro and in vivo antitumor effects of *C japonica* extracts and derived phytochemicals

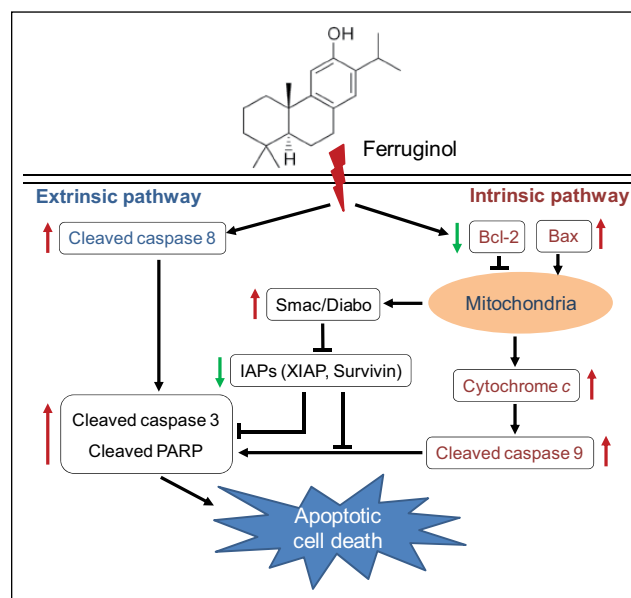


Figure 7. Proposed mechanisms of ferruginol-induced apoptosis via caspase-dependent molecular pathways in A549 and CL1-5 human non-small cell lung cancer cells.

were assessed for the first time. Ferruginol, a diterpene phytochemical that was isolated from the leaves of *C. japonica*, exhibited excellent bioactivity. The antitumor effects of ferruginol and the cellular and molecular mechanisms responsible for these actions were evaluated in the A549 and CL1-5 human NSCLC cell lines. The results of the present study revealed that ferruginol activated a caspase-dependent mitochondrial apoptotic pathway in the 2 cell lines. Intraperitoneal administration of ferruginol significantly suppressed the growth of subcutaneous CL1-5 xenografts. The findings of the present study provided insight into the molecular mechanisms underlying ferruginol-induced apoptosis in NSCLC cells, rendering this compound a potential candidate drug for the treatment of NSCLC.

Declaration of Conflicting Interests

The author(s) declared no potential conflicts of interest with respect to the research, authorship, and/or publication of this article.

Funding

The author(s) received no financial support for the research, authorship, and/or publication of this article.

References

- Siegel R, Ma J, Zou Z, Jemal A. Cancer statistics, 2014. *CA Cancer J Clin*. 2014;64:9-29.
- Herbst RS, Heymach JV, Lippman SM. Lung cancer. *N Engl J Med*. 2008;359:1367-1380.
- Pao W, Girard N. New driver mutations in non-small-cell lung cancer. *Lancet Oncol*. 2011;2:175-180.
- Deng YT, Kim JK. EGCG inhibits the invasion of highly invasive CL1-5 lung cancer cells through suppressing MMP-2 expression via JNK signaling and induces G2/M arrest. *J Agric Food Chem*. 2011;59:13318-13327.
- Liu LC, Tsao TCY, Hsu SR, et al. EGCG inhibits transforming growth factor- β -mediated epithelial-to-mesenchymal transition via the inhibition of Smad2 and Erk1/2 signaling pathways in nonsmall cell lung cancer cells. *J Agric Food Chem*. 2012;60:9863-9873.
- Schwartz AG, Prysak GM, Bock CH, Cote ML. The molecular epidemiology of lung cancer. *Carcinogenesis*. 2007;28:507-518.
- Yu HM, Liu YF, Cheng YF, Hu LK, Hou M. Effects of rhubarb extract on radiation induced lung toxicity via decreasing transforming growth factor-beta-1 and interleukin-6 in lung cancer patients treated with radiotherapy. *Lung Cancer*. 2008;59:219-226.
- Hung JY, Hsu YL, Ni WC, et al. Oxidative and endoplasmic reticulum stress signaling are involved in hydrocortisone-mediated apoptosis in human non-small cell lung cancer cells. *Lung Cancer*. 2010;68:355-365.
- Kimura Y, Sumiyoshi M. Anti-tumor and anti-metastatic actions of wogonin isolated from *Scutellaria baicalensis* roots through anti-lymphangiogenesis. *Phytomedicine*. 2013;20:328-336.
- Chen X, Pei L, Zhong Z, Guo J, Zhang Q, Wang Y. Antitumor potential of ethanol extract of *Curcuma phaeocaulis* Valetton against breast cancer cells. *Phytomedicine*. 2011;18:1238-1243.
- Yuan JM. Green tea and prevention of esophageal and lung cancers. *Mol Nutr Food Res*. 2011;55:886-904.
- Aiyer HS, Warri AM, Woode DR, Hilakivi-Clarke L, Clarke R. Influence of berry polyphenols on receptor signaling and cell-death pathways: implications for breast cancer prevention. *J Agric Food Chem*. 2012;60:5693-5708.
- Hosseinimehr SJ, Jalayer Z, Naghshvar F, Mahmoudzadeh A. Hesperidin inhibits cyclophosphamide-induced tumor growth delay in mice. *Integr Cancer Ther*. 2012;11:251-256.
- Chu ES, Sze SC, Cheung HP, Liu Q, Ng TB, Tong Y. An in vitro and in vivo investigation of the antimetastatic effects of a chinese medicinal decoction, erxian decoction, on human ovarian cancer models. *Integr Cancer Ther*. 2013;12:336-346.
- Ooi KL, Tengku Muhammad TS, Lam LY, Sulaiman SF. Cytotoxic and apoptotic effects of ethyl acetate extract of *Elephantopus mollis* Kunth. in human liver carcinoma HepG2 cells through caspase-3 activation. *Integr Cancer Ther*. 2012;13:NP1-NL13. doi:10.1177/1534735411433203.
- Chen CC, Wu JH, Yang NS, et al. Cytotoxic C35 terpenoid cryptotriene from the bark of *Cryptomeria japonica*. *Org Lett*. 2010;12:2786-2789.
- Ho ST, Tung YT, Chen YL, Zhao YY, Chung MJ, Wu JH. Antioxidant activities and phytochemical study of leaf extracts from 18 indigenous tree species in Taiwan. *Evid Based Complement Alternat Med*. 2012;2012:215959.
- Shyur LF, Huang CC, Lo CP, et al. Hepatoprotective phytochemicals from *Cryptomeria japonica* are potent modulators of inflammatory mediators. *Phytochemistry*. 2008;69:1348-1358.
- Hisayoshi K, Youji F, Michikazu O, Kouetsu T. Antifungal diterpenes from the bark of *Cryptomeria japonica* D. Don. *Holzforschung*. 2006;60:20-23.
- Imai T, Tanabe K, Kato T, Fukushima K. Localization of ferruginol, a diterpene phenol, in *Cryptomeria japonica* heartwood by time-of-flight secondary ion mass spectrometry. *Planta*. 2005;224:549-556.
- Li S, Wang P, Deng G, Yuan W, Su Z. Cytotoxic compounds from invasive giant salvinia (*Salvinia molesta*) against human tumor cells. *Bioorg Med Chem Lett*. 2013;23:6682-6687.
- Chiang YM, Liu HK, Lo JM, et al. Cytotoxic constituents of the leaves of *Calocedrus formosana*. *J Chin Chem Soc*. 2003;50:161-166.
- Ly JD, Grubb DR, Lawen A. The mitochondrial membrane potential ($\Delta\psi_m$) in apoptosis; an update. *Apoptosis*. 2003;8:115-128.
- Gottlieb E, Armour SM, Harris MH, Thompson CB. Mitochondrial membrane potential regulates matrix configuration and cytochrome c release during apoptosis. *Cell Death Differ*. 2003;10:709-717.
- Cha JD, Kim JY. Essential oil from *Cryptomeria japonica* induces apoptosis in human oral epidermoid carcinoma cells

- via mitochondrial stress and activation of caspases. *Molecules*. 2012;17:3890-3901.
26. Lin FM, Tsai CH, Yang YC, et al. A novel diterpene suppresses CWR22Rv1 tumor growth in vivo through antiproliferation and proapoptosis. *Cancer Res*. 2008;68:6634-6642.
 27. Yoshikawa K, Tanaka T, Umeyama A, Arihara S. Three abietane diterpenes and two diterpenes incorporated sesquiterpenes from the bark of *Cryptomeria japonica*. *Chem Pharm Bull*. 2006;54:315-319.
 28. Takei M, Umeyama A, Arihara S. T-cadinol and calamenene induce dendritic cells from human monocytes and drive Th1 polarization. *Eur J Pharmacol*. 2006;53:190-199.
 29. Elmore S. Apoptosis: a review of programmed cell death. *Toxicol Pathol*. 2007;35:495-516.
 30. MacFarlane M, Williams AC. Apoptosis and disease: a life or death decision. *EMBO Rep*. 2006;5:674-678.
 31. Morales A, Alvarez A, Arvelo F, Suárez AI, Compagnone RS, Galindo-Castro I. The natural diterpene ent-16 β -17 α -dihydroxykaurane down-regulates Bcl-2 by disruption of the Ap-2 α /Rb transcription activating complex and induces E2F1 up-regulation in MCF-7 cells. *Apoptosis*. 2011;16:1245-1252.
 32. Berthelet J, Dubrez L. Regulation of apoptosis by inhibitors of apoptosis (IAPs). *Cells*. 2013;2:163-187.
 33. Ouyang L, Shi Z, Zhao S, et al. Programmed cell death pathways in cancer: a review of apoptosis, autophagy and programmed necrosis. *Cell Prolif*. 2012;45:487-498.
 34. Krepela E, Dankova P, Moravcikova E, et al. Increased expression of inhibitor of apoptosis proteins, survivin and XIAP, in non-small cell lung carcinoma. *Int J Oncol*. 2009;35:1449-1462.
 35. Sausville EA, Burger AM. Contributions of human tumor xenografts to anticancer drug development. *Cancer Res*. 2008;66:3351-3354.